



up to 300 at 1 GHz [8][9];  $\mu$ machined inductors with  $Q$ 's up to 30 at 1 GHz [10]; and  $\mu$ mechanical switches with insertion losses as low as 0.1dB [11]. Although much of the interest in these “RF MEMS” devices originally derived from their amenability to on-chip integration, it is actually their potential for enhancing robustness and reducing power consumption in alternative transceiver architectures that makes them so compelling.

## 2. Micromechanical RF Devices

Table I summarizes the RF MEMS devices most useful for communications applications. Brief descriptions of each of these devices now follow.

### A. High- $Q$ Vibrating Micromechanical Resonators

Because mechanical resonances generally exhibit orders of magnitude higher  $Q$  than their electrical counterparts, vibrating mechanical resonators are essential components in communication circuits. With appropriate scaling via MEMS technology, such devices are expected to be able to vibrate over a very wide frequency range, from 1 kHz to >1 GHz, making them ideal for highly stable oscillator and low loss filtering functions at common transceiver frequencies.

The first three rows of Table I succinctly present the evolution of vibrating  $\mu$ mechanical resonator geometries over the past five years. As shown, clamped-clamped beam resonators, which are essentially guitar strings scaled down to  $\mu$ m dimensions to achieve VHF frequencies, can achieve on-chip  $Q$ 's  $\sim$ 8,000 for oscillator and filtering functions in the HF range. However, anchor losses in this specific structure begin to limit the achievable  $Q$  at higher VHF frequencies, limiting the practical range of this structure to <100 MHz when using  $\mu$ m-scale dimensions. To achieve higher frequency while retaining  $Q$ 's in the thousands and without the need for sub- $\mu$ m dimensions [12] (which can potentially degrade the power handling and frequency stability of these devices in present-day applications [13]), more balanced structures that eliminate anchor losses can be used, such as the free-free beam [6] or contour-mode disk [7] resonators in rows 2 and 3 of Table I. These resonators are expected to be able to operate at and beyond GHz frequencies when properly scaled, all while retaining sufficiently large dimensions to maintain adequate power handling and to avoid “scaling-induced” phenomena, such as mass-loading or temperature fluctuation noise, that can begin to degrade performance when dimensions become too small [13].

Although stand-alone vibrating  $\mu$ mechanical resonators are themselves applicable to local oscillator synthesizer applications in transceivers, their application range can be greatly extended by using them in circuit networks. In particular, by interlinking mechanical elements in specific networks, a variety of low-loss circuit functions are available, from band-pass filters [5] to mixers [15] to gain devices [15]. Figure 1 presents the scanning electron micrograph (SEM) and measured frequency characteristic for a 7.81-

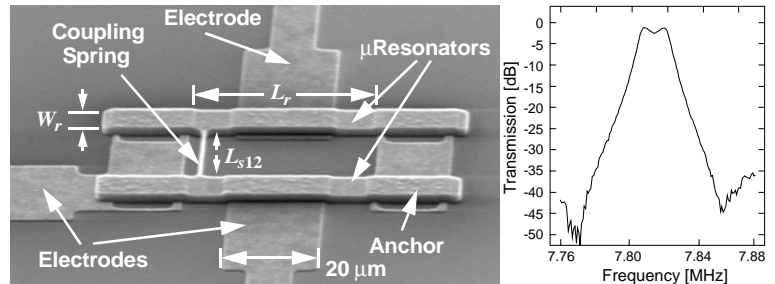


Fig. 1: SEM and measured frequency characteristic for a three-link, 7.81-MHz polysilicon  $\mu$ mechanical filter [5].

MHz polysilicon surface-micromachined  $\mu$ mechanical filter that measures only  $40\mu\text{m}\times 30\mu\text{m}$ , and that shows only 1 dB of insertion loss for a 0.22% bandwidth, all attained with zero dc power consumption. Beyond its tiny size and superb frequency shaping ability, the micromechanical filter of Fig. 1 is also on/off switchable via mere charging and discharging of its conductive vibrating structure, making it an ideal candidate for use in switchable high- $Q$  filter banks for multi-band reconfigurable transceiver applications [1]-[3].

### B. High- $Q$ Tunable Capacitors

Tunable  $\mu$ mechanical capacitors, summarized in row 4 of Table I, consist of metal plates that can be electrostatically moved with respect to one another, allowing voltage-control of the capacitance between the two plates. Because metal materials can be used in their construction,  $Q$ 's as high as 300 can be attained [9]—much higher than attainable by lossy semiconductor pn diodes offered by conventional IC technology. Paired with medium- $Q$  inductors,  $\mu$ mechanical capacitors can enhance the performance of low noise VCO's. Also, if inductors could also be achieved with  $Q$ 's as high as 300, tunable RF pre-select filters might be attainable that could greatly simplify the implementation of multi-band transceivers.

### C. Medium- $Q$ Micromachined Inductors

As mentioned above, tunable  $\mu$ mechanical capacitors must be paired with inductors with  $Q > 20$  to be useful in communication circuits. Unfortunately, due to excessive series resistance and substrate losses, conventional IC technology can only provide spiral inductors with  $Q$ 's no higher than 7. Using MEMS technologies to both thicken metal turns (reducing series resistance) and suspend the inductor turns away from the substrate (reducing substrate losses), inductors with  $Q$ 's as high as 30 at 1 GHz have been demonstrated (c.f., row 5 of Table I) [10]. Although not the  $Q \sim 300$  needed for multi-band tunable RF filters, this  $Q \sim 30$ , when paired with a  $\mu$ mechanical capacitor, should allow the implementation of low noise VCO's with lower power consumption than those using conventional IC technology [14]. Tunable bias/matching networks that can reduce power consumption in power amplifiers should also be feasible.

### D. Micromechanical Switches

Micromechanical switches [11] have essentially the same structure as the clamped-clamped beam resonators of row 1 in Table I, but are operated in a binary fashion: when the beam is up, the switch is open; when the beam is pulled down (e.g., by an electrostatic force), the switch is closed. Again, due to their metal construction made possible by MEMS technology,  $\mu$ mechanical switches post much smaller insertion losses than their FET-based counterparts (0.1 dB versus 2 dB) and are many times more linear, with  $IIP_3$ 's  $> 66$  dBm. Although their switching times are much slower than that of FETs, they are still adequate for antenna switching, switchable filter, and phased array antenna applications, provided their high switching voltage levels can be reduced or accommodated. If achievable, the above applications are desirable for multi-band reconfigurability in handsets and for diversity against multi-path fading. At present, the industry awaits improvements in the reliability of  $\mu$ mechanical switches.

## 3. MEMS-Based Transceiver Architectures

Perhaps the most direct way to harness RF MEMS devices is via direct replacement of off-chip components, as shown in Fig. 2. Due mostly to the higher  $Q$  attainable by on-chip  $\mu$ mechanical vibrating resonators relative to off-chip counterparts, analyses before and after replacement by MEMS in a super-heterodyne architecture often show dramatic improvements in receiver noise figure, e.g., from 8.8 dB to 2.8 dB.

Although beneficial, the performance gains afforded by mere direct replacement by MEMS are quite limited when compared to more aggressive uses of MEMS technology. To fully harness the advantages of  $\mu$ mechanical circuits, one should take advantage of their micro-scale size and zero dc power consumption, and use them in massive quantities to enhance robustness and trade  $Q$  for power consumption. Figure 3 presents the system-level block diagram for a possible transceiver front-end architecture that takes full advantage of the complexity achievable via  $\mu$ mechanical circuits [1][2]. The main driving force behind this architecture is power reduction, attained in several of the blocks by replacing active components by low-loss passive  $\mu$ mechanical ones, and by trading power for high selectivity (i.e., high- $Q$ ). Among the key performance enhancing features are: (1) an RF channel selector comprised of a bank of switchable  $\mu$ mechanical filters, offering multi-band reconfigurability, receive power savings via relaxed dynamic range requirements [3], and transmit power savings by allowing the use of a more efficient power amplifier; (2) use of a passive  $\mu$ mechanical mixer-filter to replace the active mixer normally used, with obvious power savings; (3) a VCO referenced to a switchable bank of  $\mu$ mechanical resonators, capable of operating without the need for locking to a lower frequency reference, hence, with orders of magnitude lower power consumption than present-day synthesizers; (4) use of a  $\mu$ mechanical T/R switch, with the potential for large power savings in transmit-mode; and (5) use of  $\mu$ mechanical resonator and switch components around the power amplifier to enhance its efficiency.

Although already quite aggressive, the architecture of Fig. 3 may still not represent the best power savings afforded by MEMS. In fact, even more power savings than in Fig. 3 are possible if the high- $Q$   $\mu$ mechanical circuits in the signal path can post such low losses that the RF LNA (normally required to boost the received signal against losses and noise from subsequent stages) may in fact no longer be needed. Rather, the RF LNA can be removed, and

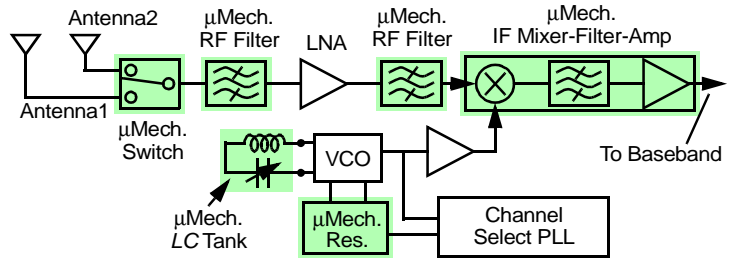


Fig. 2: System block diagram of a super-heterodyne receiver architecture showing potential replacements via MEMS-based components. (On-chip  $\mu$ mechanics are shaded.)

the needed gain to baseband provided instead by an IF LNA that consumes much less power since it operates at the much lower IF frequency. Without the RF LNA or transistor mixer, the receiver front-end architecture reduces to an all-MEMS topology, such as shown in Fig. 4. Here, since the absence of RF transistor circuits removes dynamic range concerns, the channel-selecting filter bank of Fig. 3 has been converted to a mixer-filter bank and moved down to the IF frequency, where it might be easier to implement, and where it allows the use of a single-frequency RF local oscillator (LO) to down-convert from RF to IF. Since the RF LO is now a single frequency oscillator, power hungry phase-locking and pre-scaling electronics are not needed, allowing similar power advantages as for the VCO in the architecture of Fig. 3. In fact, the architecture of Fig. 4 attains all the power advantages of that of Fig. 3, plus additional power savings due to the lack of an LNA. It, however, does so at the cost of a slightly higher overall noise figure and decreased robustness against hostile (i.e., jamming) interferers versus Fig. 3.

#### 4. Conclusions

Micromechanical circuits attained via MEMS technologies have been described that can potentially play a key role in removing the board-level packaging requirements that currently constrain the size of communication transceivers. In addition, by combining the strengths of integrated  $\mu$ mechanical and transistor circuits, using both in massive quantities, previously unachievable functions become possible that may soon enable alternative transceiver architectures with substantial performance gains, especially from a power perspective. To reap the benefits of these new architectures, however, further advancements in device frequency, linearity, and manufacturability are required [1]. Research efforts are ongoing.

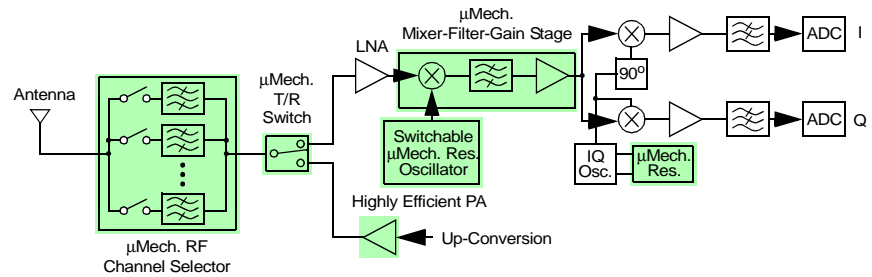


Fig. 3: System block diagram for an RF channel-select receiver architecture utilizing large numbers of micromechanical resonators in banks to trade  $Q$  for power consumption. (On-chip  $\mu$ mechanics are shaded.)

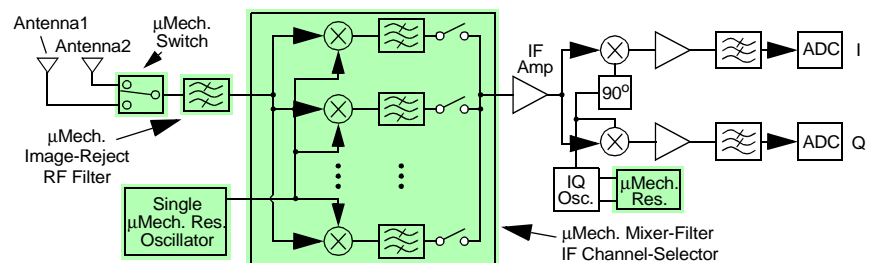


Fig. 4: System block diagram for an all-MEMS receiver front-end, employing an RF image-reject filter, a fixed  $\mu$ mechanical resonator local oscillator, and a switchable array of IF  $\mu$ mechanical mixer-filters.

**Acknowledgment.** The author is grateful for research support from DARPA and from NSF.

#### References.

- [1] C. T.-C. Nguyen, 2000 Bipolar/BiCMOS Ckts. and Tech. Mtg (BCTM), Sept. 25-26, 2000, pp. 142-149.
- [2] C. T.-C. Nguyen, Topical Mtg. on Silicon Monolithic IC's in RF Systems, Sept. 12-14, 2001, pp. 23-32.
- [3] C. T.-C. Nguyen, *IEEE Trans. Microwave Theory Tech.*, vol. 47, no. 8, pp. 1486-1503, Aug. 1999.
- [4] C. T.-C. Nguyen, L. P.B. Katehi, and G. M. Rebeiz, *Proc. IEEE*, vol. 86, no. 8, pp. 1756-1768, Aug. 1998.
- [5] F. D. Bannon III, *et al.*, *IEEE J. Solid-State Circuits*, vol. 35, no. 4, pp. 512-526, April 2000.
- [6] K. Wang, *et al.*, *IEEE/ASME J. Microelectromech. Syst.*, vol. 9, no. 3, pp. 347-360, Sept. 2000.
- [7] J. R. Clark, *et al.*, 2000 IEEE Int. Electron Devices Mtg (IEDM), Dec. 11-13, 2000, pp. 399-402.
- [8] D. J. Young, *et al.*, 1996 Solid-State Sensor and Actuator Workshop, June 2-6, 1996, pp. 86-89.
- [9] J.-B. Yoon, *et al.*, 2000 IEEE Int. Electron Devices Meeting (IEDM), Dec. 11-13, 2000, pp. 489-492.
- [10] J. B. Yoon, *et al.*, 1999 IEEE Int. Electron Devices Mtg (IEDM), Dec. 5-8, 1999, pp. 753-756.
- [11] Z. J. Yao, *et al.*, *IEEE/ASME J. Microelectromech. Syst.*, pp. 129-134, June 1999.
- [12] M. L. Roukes, 2000 Solid-State Sensor and Actuator Workshop, June 4-8, 2000, pp. 367-376.
- [13] J. R. Vig, *et al.*, *IEEE Trans. Ultrason. Ferroelec. Freq. Contr.*, vol. 46, no. 6, pp. 1558-1565, Nov. 1999.
- [14] A. Dec, *et al.*, *IEEE J. Solid-State Circuits*, vol. 35, no. 8, pp. 1231-1237, Aug. 2000.
- [15] A.-C. Wong, *et al.*, 1998 IEEE Int. Electron Devices Meeting (IEDM), Dec. 6-9, 1998, pp. 471-474.